SUPPLEMENTAL DATA for

RNA recognition by minimal ProQ from *Neisseria meningitidis*

Maciej Basczok and Mikołaj Olejniczak

SUPPLEMENTAL MATERIALS AND METHODS

ProQ-binding assay

The RNA binding to ProQ protein was measured using a gelshift assay as described in the Materials and Methods section in the main text.

Analysis of RNA sequences

To compare the nucleotide composition of the sequence 5′-adjacent to the terminator stem, we used data from global profiling studies using CLIP-seq for *N. meningitidis* ProQ (Bauriedl et al. 2020) and using RIP-seq for *N. meningitidis* Hfq (Heidrich et al. 2017). For the analysis, we selected 40 3′-UTRs and sRNAs, which were the top ligands containing Rho-independent terminators of each protein (Suppl. Fig. S6). In CLIP-seq data for ProQ-bound RNAs only those RNAs were selected, in which the peak at least partially covered a terminator hairpin. In RIP-seq data for Hfq-bound RNAs all RNAs annotated as 3' UTRs or sRNAs were considered in the analysis. In these RNA ligands, a 10-nt long sequence 5′-adjacent to the intrinsic terminator was analyzed. To define the sequences 5'-adjacent to the terminator hairpins the secondary structure of each RNA was analyzed using the *ViennaRNA* package (Lorenz et al. 2011). The 3' end of this sequence was defined as the nucleotide located immediately on the 5' side of the closing G-C/C-G pair of the terminator stem.

The extracted 10-nt long sequences were then used to generate the sequence logos with *WebLogo* (Crooks et al. 2004). RNA sequences selected for analysis are shown in Supplemental Table S4.

Analogous analysis was carried out for a random gene sample of 98 genes from the *Neisseria meningitidis* transcriptome. Subsequently, the statistical importance of nucleotide frequency at each position of the 10-nt sequence 5'-adjacent to the terminator hairpin in the RNA ligands of ProQ was calculated in reference to the RNA ligands of Hfq and the random gene sample using the *pLogo* software (O'Shea et al. 2013).

To classify ProQ RNA ligands according to their intrinsic terminator characteristics (Suppl. Fig. S1), CLIP-seq peaks (Bauriedl et al. 2020) were mapped to the *Neisseria meningitidis* 8013 genome, and extended by 30 nucleotides in both upstream and downstream directions. Secondary structure for each RNA sequence was predicted with *ViennaRNA* package (Lorenz et al. 2011) and manually inspected for Rho-independent transcription terminator presence and features.

Statistical analysis

As a comparison to non-linear regression analysis used to obtain average K_d values and standard deviations for each binding reaction, which are reported in Tables 1 - 6 of the main text, we also performed global regression fitting of the binding data for all replicates (Suppl. Table S5). In global data fitting we used quadratic equation for all datasets, except for AniS-loop and AniS-3UtoA constructs, where we used the Hill equation. This analysis was followed by Z-score calculation and statistical significance determination. Non-linear regression fits were performed in *GrapPad Prism* 10.3.1, and the following statistical analysis was carried out in R.

SUPPLEMENTAL TABLES

Supplemental Table S1. The calculation of K_d values using global fitting and the analysis of statistical significance of observed differences between mutant and unmodified RNAs.

Figure Table	name	average K_d [nM]	SD	global K_d	K_d diff	bottom CI	upper CI	SE	Z-score	p-value
Fig. 1C (Table 1)	AniS-3'	5	0.4	5	0	3.8	6.4	-	-	-
	Bns1	0.65	0.54	0.52	0.13	0.31	0.8	-	-	-
	carA-5'	1.3	0.42	1.2	0.1	0.96	1.6	-	-	-
	iga-3'	0.3	0.28	0.17	0.13	0.00	0.57	-	-	-
	intergenic	1.4	1	1.1	0.3	0.69	1.6	-	-	-
	pnp-5'	7.9	0.8	2	5.9	0.96	3.7	-	-	-
	rpmG-3'	1	0.52	0.95	0.05	0.65	1.3	-	-	-
Fig. 2B (Table 2)	*rpmG*-U_6AU_2	0.22	0.26	0.17	0.03	0.08	0.3	0.056	-4.2	2.36E-05*
	rpmG-U_6AU	0.2	0.23	0.05	0.15	0.002	0.13	0.031	-5	4.65E-07*
	rpmG-U_6A	< 0.5	-	0.01	-	0	0.1	0.025	-5.3	1.22E-07*
	***rpmG*-3'**	1	0.52	0.95	0.05	0.65	1.3	0.18	-	-
	rpmG-U_5	0.47	0.27	0.62	-0.15	0.48	0.78	0.077	-1.7	0.08
	rpmG-U_4	2.6	3.5	1.2	1.4	0.5	2.4	0.48	0.45	0.65
Fig. 2D (Table 2)	**AniS-3'**	5	0.4	5	0	3.8	6.6	0.72	-	-
	AniS-U_7	0.82	0.21	0.81	-0.01	0.6	1.1	0.12	-5.8	6.26E-09*
	AniS-U_6	0.7	0.62	0.51	0.19	0.26	0.89	0.16	-6.1	7.96E-10*
	AniS-U_5	6.5	1.3	6.3	0.2	4.7	8.2	0.85	1.1	0.25
	AniS-U_4	0.9	0.58	0.73	0.17	0.32	1.4	0.27	-5.6	2.04E-08*
Fig. 3B (Table 3)	*rpmG*-3'	1	0.52	0.95	0.05	0.65	1.3	0.18	-3.3	9.69E-04
	***rpmG*-45**	2.8	1.7	2.2	0.6	1.6	3	0.34	-	-
	rpmG-35	0.84	0.23	0.84	0	0.64	1.1	0.11	-0.54	0.59
	rpmG-33	7.3	2.5	6.8	0.5	5.2	8.7	0.89	6.43	1.28E-10*
Fig. 3D (Table 3)	AniS-3'	5	0.4	5	0	3.8	6.6	0.72	1.2	0.22
	AniS-40	3.9	4.4	4.6	-0.7	3.1	6.7	0.90	-0.62	0.53
	AniS-37	3.9	1.2	4	-0.1	3	5.1	0.54	-	-
Fig. 4B (Table 4)	*rpmG*-3'	1	0.52	0.95	0.05	0.65	1.3	0.18	2.2	0.031*
	***rpmG*-loop**	0.5	0.34	0.5	0	0.31	0.75	0.11	-	-
	rpmG-loop-44	4	2	3.6	0.4	2.7	4.8	0.54	5.7	1.52E-08*
	rpmG-loop-40	1.2	1.5	2	-0.8	0.67	4.6	1	1.4	0.15
	rpmG-loop-36	0.13	0.14	0.12	0.01	0.01	0.34	0.084	-2.7	6.7E-03*
Fig. 4D (Table 4)	AniS-3'	5	0.4	5	0	3.8	6.6	0.72	5.4	6.95E-08*
	AniS-loop	0.39	0.18	0.04	0.35	0.01	0.17	0.04	-4.5	6.66E-06*
	AniS-loop-39	1.1	1.1	1	0.1	0.66	1.5	0.21	-	-
	AniS-loop-35	1	0.31	0.98	0.02	0.76	1.3	0.13	-0.082	0.93
	AniS-loop-31	8.3	3.7	6.9	1.4	5.4	8.7	0.85	6.7	2.40E-11*
	AniS-loop-29	5.8	3.9	4.7	1.1	3.4	6.6	0.82	4.4	9.59E-06*
	AniS-loop-27	4.4	2.8	3.6	0.8	2.4	5.5	0.80	3.2	0.0014*
Fig. 5B (Table 5)	**AniS-37**	3.9	1.2	4	-0.1	3	5.1	0.54	-	-
	AniS-C	11	6.9	8	3	4.3	14.7	2.66	1.5	0.14

Figure Table	name	average K_d	SD	global K_d	K_d diff	bottom CI	upper CI	SE	Z-score	p-value
Fig. 6B (Table 6)	***rpmG*-3'**	1	0.52	0.95	0.5	0.65	1.3	0.18	-	-
	rpmG-2AtoU	1.7	0.81	1.6	0.89	1.2	2.2	0.27	2.08	0.034*
	rpmG-3AtoU	4.2	2.7	3.5	1.5	2.2	5.3	0.79	3.11	1.8E-3*
Fig. 6D (Table 6)	**AniS-3'**	5	0.4	5	0	3.8	6.6	0.72	-	-
	AniS-2UtoA	2.8	0.55	2.8	0	2.2	3.4	0.31	-2.9	0.0034*
	AniS-3UtoA	0.3	0.073	0.3	0	0.27	0.33	0.015	-6.6	4.5E-11*

Global K_d values were obtained by performing non-linear regression on all replicates simultaneously. The data were fit using the quadratic equation except for the data for AniS-loop and AniS-3UtoA constructs, which were fit using the Hill equation. K_d diff – difference between average and global K_d values, bottom CI – bottom confidence interval value, upper CI - upper confidence interval value, SE – standard error. **Bold** – reference reaction, * - statistical significance (p-value < 0.05). Binding reactions in which maximum fraction bound was lower than 40% (Tables 1-5) were not included in this analysis. Data for average K_d and its standard deviation are taken from Tables 1-6 from the main text.

Supplemental Table S2. 10 nt sequences on the 5' side of the closing G-C/C-G pair of terminator stems of ProQ- and Hfq-specific RNAs, which were used for the sequence logo analysis.

Top 40 *N. meningitidis* ProQ ligands CLIP-seq dataset (Bauriedl et al. 2020)	sequence	Top 40 *N. meningitidis* Hfq ligands RIP-seq dataset (Heidrich et al. 2017)	sequence
intergenic, 2094444-2094518(-)	AUGCCGAAAG	NMV_1189 3'	UUGAAACAAU
iga 3'	AAAAUAAAAU	recC 3'	AAAGGCAAAU
NMV_1592 3'	AUAAGGCAAU	uvrB 3'	GAGUAAUAAA
comE1 3'	CGCAUCAAAU	recR 3'	AAUGCAAAAU
NMnc0006	ACUACACAAA	NMV_1052 3'	UCUGGAAAAU
nuoN 3'	GCCGCCGCAA	prmB 3'	AAGGGGAAAU
NMV_1266 3'	AUCCGAACAA	RcoF1	UGUAGACUUG
nrdB 3'	UUGAAAAAAU	RcoF2	UGUAGACUUG
pilX 3'	UUUUGCCAAU	Int 3'	AGUGAUACCU
alx 3'	AAACAAAAAA	lpxA 3'	GCUGACCGUA
NMV_0646 3'	GUUAUGAAAA	NMV_1503 3'	UUUGUAUUAU
nagZ 3'	CAUAUUCAAA	NMV_1295 3'	CGAUUCUAAG
NMV_0508 3'	CAUUAAAAAU	NMV_0065 3'	UGAAAAAAAA
panC 3'	CGUCGGGAAU	NMV_2316 3'	AGCUAGGUAA
queA 3'	GAAGACAAGU	NMV_1651 3'	GUUCCUUUUG
intergenic, 765600-765668(-)	AAUAUCAAAG	NMV_2146 3'	UAUCUGCAAA
intergenic, 1916777-1916862(-)	GUUAAAAAAU	NMV_0065 3'	GAAGACAAGU
NMnc0041	UUGGGGGGAA	NMnc0041	UUGGGGGGAA
dnaN 3'	UGGAGAUAUA	NMV_0057 3'	CGCAUCAAAU
gloA 3'	CGCCGCCAAU	NMV_0638 3'	UUGAACGAAU
rplI 3'	AUUAUCAGAU	NMV_0320 3'	UAAUUUAAAA
NMV_0480 3'	GCAUCAAAAU	NMV_1804 3'	AAGCGCAUAU
NMV_0949 3'	UCGCAAAAAU	sigEsRNA	UCCUUGGGAA
purM 3'	AUAGCGAAAU	AniS	UGUGUGUUUU
NMV_2143 3'	CAUUGAAAAU	NMV_1296 3'	AGAAUGGAAU
carA 3'	GCCCGAAAAG	NMV_0692 3'	UAAGUCAAAA
dsbA2 3'	AAUGAGUAAA	NMV_0091 3'	UGACGGAAAU
NMV_0786 3'	AGCCCGAUAU	ppsA 3'	CAAUGCCCAU

intergenic, 1193850-1193917(+)	CAAAACAUAA	NMV_0441 3'	UUGACAGAAU
rplY 3'	GUUGUUUUAU	NMV_1746 3'	UUUGAUUAAA
dsbD 3'	UGUUUCAAAU	NMV_1201 3'	CGAUAAAAAA
atpC 3'	GUUUGGAAAA	rplS 3'	UUCCCCCAAU
intergenic, 2203594-2203659(-)	CCCAGAUAAA	NMV_1560 3'	AACGGCAAAU
NMV_0791 3'	GGAUUGAAAU	NMV_1509 3'	UUUUGCCAAU
NMnc0044	GAAGACAAGU	NMV_2134 3'	CGGAAAAGGU
NMV_1640 3'	GUAAAAAAAU	NMV_0716 3'	AACCAUAAAG
dnaJ 3'	CGGAAACAAG	recA 3'	UCCCGAUAAA
prc 3'	UUUUUACGAU	dnaK 3'	UCUGAAAAAA
comP 3'	UUCGCCACUU	NMV_1336 3'	UUUUUGAAAU
intergenic, 2167518-2167594(+)	AAAUAUCAAA	bfr 3'	CAUCAUCAGA

Supplemental Table S3. DNA oligonucleotides used to prepare the insert to clone *Neisseria meningitidis proQ* gene into the pET-15b expression plasmid.

name	sequence (5' → 3')
Nm-ProQ-F	cggc**ggatcc**g**gaaaatctttatttccaatcc**ATGACACAAGAAACCGCTTTGGGTGC
Nm-ProQ-R	cggc**ggatcc**TTATTCTGCTGCGGAAGATTCGGCTGC

cggc - sequence inserted to improve the efficiency of BamHI cleavage

ggatcc - BamHI restriction site

gaaaatctttatttccaatcc - sequence encoding amino acid sequence recognised by protease TEV (ENLYFQ↓S)

Supplemental Table S4. Oligonucleotides used to prepare templates for *in vitro* transcription in primer extension reaction.

name	sequence (5' → 3')
AniS-2UtoA-F	**TAATACGACTCACTATA**GGTTTCCTCTTGATGTGTGTGTGTAAGGGTGTGG
AniS-2U-R	AAGGGGTGGCGGCAGCCACACCCAAACACACACAC
AniS-2UtoA-R	AAAAAAAAGGGGTGGCGGCAGCCACACCCTTACACACACAC
AniS-3UtoA-F	**TAATACGACTCACTATA**GGTTTCCTCTTGATGTGTGTGTGAAAGGGTGTGGCTGC
AniS-3UtoA-R	AAAAAAAAGGGGTGGCGGCAGCCACACCCTTTCACAC
AniS-3'-F	**TAATACGACTCACTATA**GTTTCCTCTTGATGTGTGTGTGTTTGGGTGTGG
AniS-3'-R	AAAAAAAAGGGGTGGCGGCAGCCACACCCAAACACACACAC
AniS-noU-R	GGGGTGGCGGCAGCCACACCCAAACACACACAC
AniS-U2-R	AAGGGGTGGCGGCAGCCACACCCAAACACACACAC
AniS-U4-R	AAAAGGGGTGGCGGCAGCCACACCCAAACACACACAC
AniS-U5-R	AAAAAGGGGTGGCGGCAGCCACACCCAAACACACACAC
AniS-U6-R	AAAAAAGGGGTGGCGGCAGCCACACCCAAACACACACAC
AniS-U7-R	AAAAAAAGGGGTGGCGGCAGCCACACCCAAACACACACAC
Bns1-F	**TAATACGACTCACTATA**GGACAAGTCCAAGTATTATAAAGGCTGAATAAAGAGGAAACAGCAGGCAGATATA
Bns1-R	AAAAAAGCAGATATATTCGGACTGCACCTCCCGAATATATCTGCCTGCTGTTTCC
carA-5'-F	**TAATACGACTCACTATA**GGGTATAGGCACTTGCCCGAAAAGCACGTTACG
carA-5'-R	AAAAAAAAACACGCCGCGCAAGATAGACGCGTAACGTGCTTTTCGGGCA
iga-3'-F	**TAATACGACTCACTATA**GAAAATACTAAATTCATAGCAAAATAAAATGCCGTCTGA
iga-3'-R	ATAAAAATGCCGTCTGAAGCCTGAGTTCAGACGGCATTTTATTTTG
intergenic-F	**TAATACGACTCACTATA**GGATATGCCGAAAGGGGTTTGACGATGCCGCCGTGCGCTGTC
intergenic-R	AGAAAAAGGGTTTGACAGCGCACGGCGGCATCG
pnp-3'ext-F	**TAATACGACTCACTATA**GTTTACAACCTGCCGCACGGTCTGAAACCCTAACTATGCACATTCGGATTTTA
pnp-3'ext-R	TATTGTTCCTTTCAAAATACCGCACTGCTAAAACACTAATAATGCACACTAAAATCCGAATGTGCATAG
pnp-5'-F	**TAATACGACTCACTATA**GTTTACAACCTGCCGCACGGTCTGAAACCCTAACTATG
pnp-5'-R	AATAATGCACACTAAAATCCGAATGTGCATAGTTAGGGTTTCAGACC
rpmG-2AtoU-F	**TAATACGACTCACTATA**GGGATTTCAGTTTGAAAGCATTGCCTCCGA
rpmG-2AtoU-R	AAAAAAGCCTCCGAACAGTCGGAGGCAATGCTTTCAAA
rpmG-31-F	**TAATACGACTCACTATA**GCAAAGCCTCCGACTGTTC
rpmG-31-R	AAAAAAGCCTCCGAACAGTCGGAGGCTTTGC
rpmG-33-F	**TAATACGACTCACTATA**GAGCAAAGCCTCCGACTGTTC

rpmG-35/33-R	AAAAAAGCCTCCGAACAGTCGGAGGCTTTGCTT
rpmG-35-F	**TAATACGACTCACTATA**GAAAGCAAAGCCTCCGACTGTTC
rpmG-36-loop-F	**TAATACGACTCACTATA**GGGATTTCAGTTTGAAAGCAAAGCGAAAG
rpmG-36-loop-R	AAAAAAGCTTTCGCTTTGCTTTCAAAC
rpmG-3AtoU-F	**TAATACGACTCACTATA**GGGATTTCAGTTTGAAAGCTTTGCCTCCGA
rpmG-3AtoU-R	AAAAAAGCCTCCGAACAGTCGGAGGCAAAGCTTTCAAA
rpmG-3UtoA-R	AAATAAGCCTCCGAACAGTCGGAGGCTTTGC
rpmG-3'ext-R	ATAAAAATAAAAAAGCCTCCGAACAGTCGGAGGCTTTGCTTTCAAA
rpmG-3'-F	**TAATACGACTCACTATA**GGGATTTCAGTTTGAAAGCAAAGCCTCCGA
rpmG-3'-R	AAAAAAGCCTCCGAACAGTCGGAGGCTTTGCTTTCAAA
rpmG-40-loop-F	**TAATACGACTCACTATA**GGGATTTCAGTTTGAAAGCAAAGCCTGAAAAGG
rpmG-40-loop-R	AAAAAAGCCTTTTCAGGCTTTGCTTTC
rpmG-44-loop-F	**TAATACGACTCACTATA**GGGATTTCAGTTTGAAAGCAAAGCCTC
rpmG-44-loop-R	AAAAAAGCCTCCTTTCGGAGGCTTTGCTTTCAAACTG
rpmG-7U6A-R	TAAAAAAGCCTCCGAACAGTCGGAGGCTTTGCTTTCAAA
rpmG-95-F	**TAATACGACTCACTATA**GATCCGGTTGCCCGCAAACACGTAGTGTACAAAGAAACCAAACTGAAATAATTT
rpmG-F	**TAATACGACTCACTATA**GGGATTTCAGTTTGAAAGCAAAGCCTCCGA
rpmG-loop-F	**TAATACGACTCACTATA**GGGAUUUCAGUUUGAAAGCAAAGCCUCCGAGAA
rpmG-loop-R	GAAAGCAAAGCCUCCGAGAAAUCGGAGGCUUUUUU
rpmG-noU-R	GCCTCCGAACAGTCGGAGGCTTTGCTTTCAAA
rpmG-R	AAAAAAGCCTCCGAACAGTCGGAGGCTTTGCTTTCAAA
rpmG-U2	AAGCCTCCGAACAGTCGGAGGCTTTGCTTTCAAA
rpmG-U4-R	AAAAGCCTCCGAACAGTCGGAGGCTTTGCTTTCAAA
rpmG-U5-R	AAAAAGCCTCCGAACAGTCGGAGGCTTTGCTTTCAAA
rpmG-U6AU2-R	AATAAAAAAGCCTCCGAACAGTCGGAGGCTTTGCTTTCAAA
rpmG-U6AU-R	ATAAAAAAGCCTCCGAACAGTCGGAGGCTTTGCTTTCAAA
rpmG-UtoA-F	**TAATACGACTCACTATA**GGGATTTCAGTTTGAAAGCAAAGCCTCCGACTG
sodC-3'ext-R	ATATCTAGCAAAAAAGTGCGGTCAAAATTCACCGCACTTTTCGTTTCGAACA
sodC-3'-F	**TAATACGACTCACTATA**GATTAAATAATTCGATTGTTCGAAACGAAAAGTGCG
sodC-3'-R	AAAAAAGTGCGGTCAAAATTCACCGCACTTTTCGTTTCGAACA

The **bold font** is the sequence of T7 polymerase promoter.

Supplemental Table S5. Oligoribonucleotides obtained by chemical synthesis (Metabion)

name	**sequence (5' → 3')**
AniS-23	UGUGUGUGUUUGAAAUUUUUUUU
AniS-25	UGUGUGUGUUUGGAAACUUUUUUUU
AniS-29	GGGUGUGGCUGCCGCCACCCCUUUUUUUU
AniS-31	UUGGGUGUGGCUGCCGCCACCCCUUUUUUUU
AniS-33	GUUUGGGUGUGGCUGCCGCCACCCCUUUUUUUU
AniS-35	GUGUUUGGGUGUGGCUGCCGCCACCCCUUUUUUUU
AniS-37	GUGUGUUUGGGUGUGGCUGCCGCCACCCCUUUUUUUU
AniS-40	UGUGUGUGUUUGGGUGUGGCUGCCGCCACCCCUUUUUUUU
AniS-loop	UGUGUGUGUUUGGGUGUGGCGAAAGCCACCCCUUUUUUUU
AniS-loop-27	UGUGUGUGUUUGGGAAACCUUUUUUUU
AniS-loop-29	UGUGUGUGUUUGGGGAAACCCUUUUUUUU
AniS-loop-31	UGUGUGUGUUUGGGGGAAACCCCUUUUUUUU
AniS-loop-35	UGUGUGUGUUUGGGGUGGAAACACCCCUUUUUUUU
AniS-loop-39	UGUGUGUGUUUGGGGUGGCGAAAGCCACCCCUUUUUUUU
rpmG-26	GCCUCCGACUGUUCGGAGGCUUUUUU
rpmG-29	AAAGCCUCCGACUGUUCGGAGGCUUUUUU
rpmG-45	AUUUCAGUUUGAAAGCAAAGCCUCCGACUGUUCGGAGGCUUUUUU

SUPPLEMENTAL FIGURES

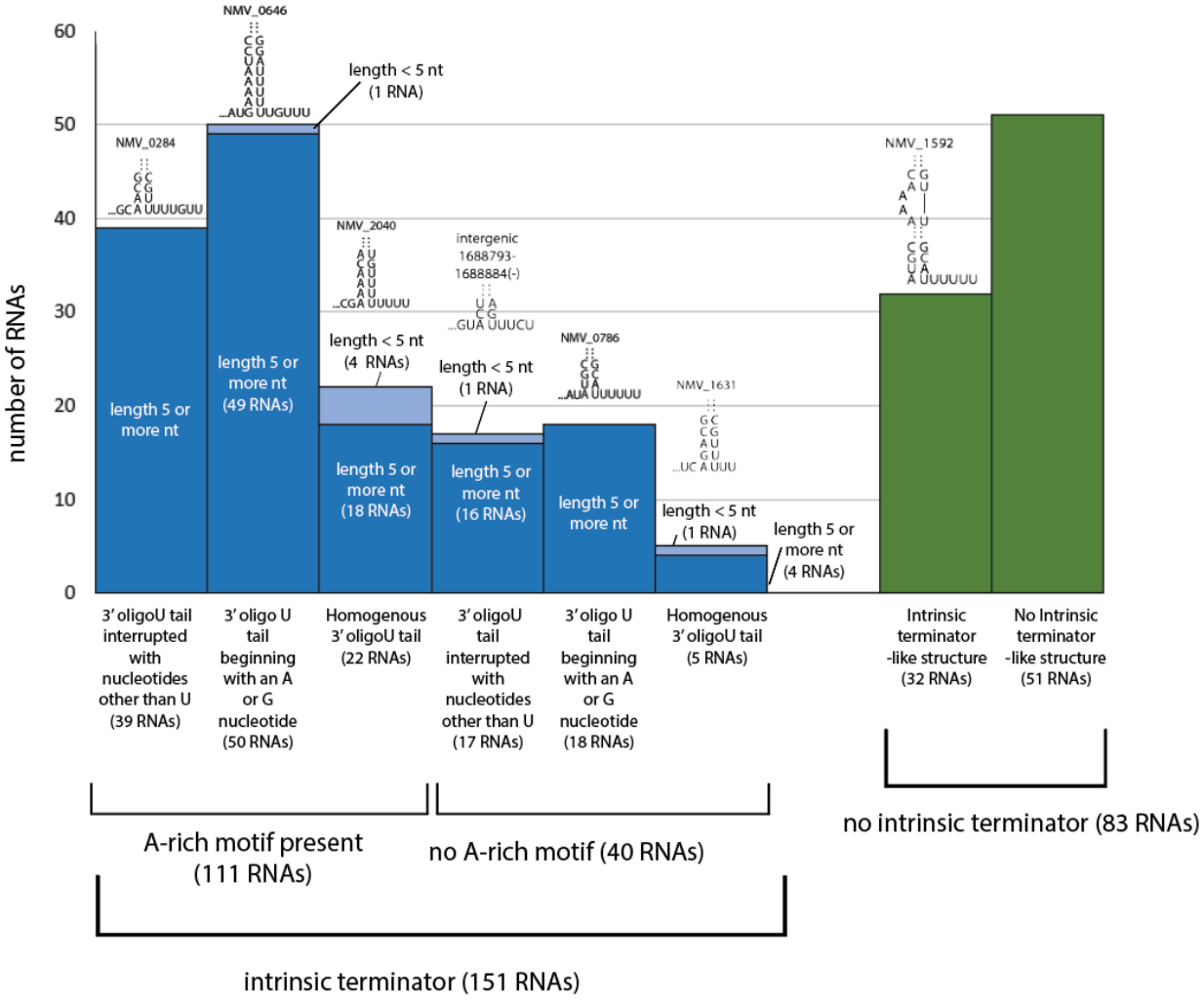

Supplemental Figure S1. Structure classification of the 3' termini of *Neisseria meningitidis* ProQ RNA ligands. *Neisseria meningitidis* ProQ-bound RNAs were classified in terms of intrinsic terminator characteristics. The description of classification criteria marked on the figure: intrinsic terminator present – a CLIPseq peak (Bauriedl et al. 2020) at least partially covered a stable hairpin followed by a 3′ tail composed mostly of uridines; A-rich motif present - a sequence of at least 2 As was present immediately on the 5′ side of the closing G-C/C-G pair of the terminator hairpin; homogenous 3′ tail – an undisrupted stretch of uridines was located at the RNA's 3′ end (starting with uridine); terminator-like structure – secondary structure consisting of a hairpin followed by an U-enriched sequence, which is not known to serve as an intrinsic terminator.

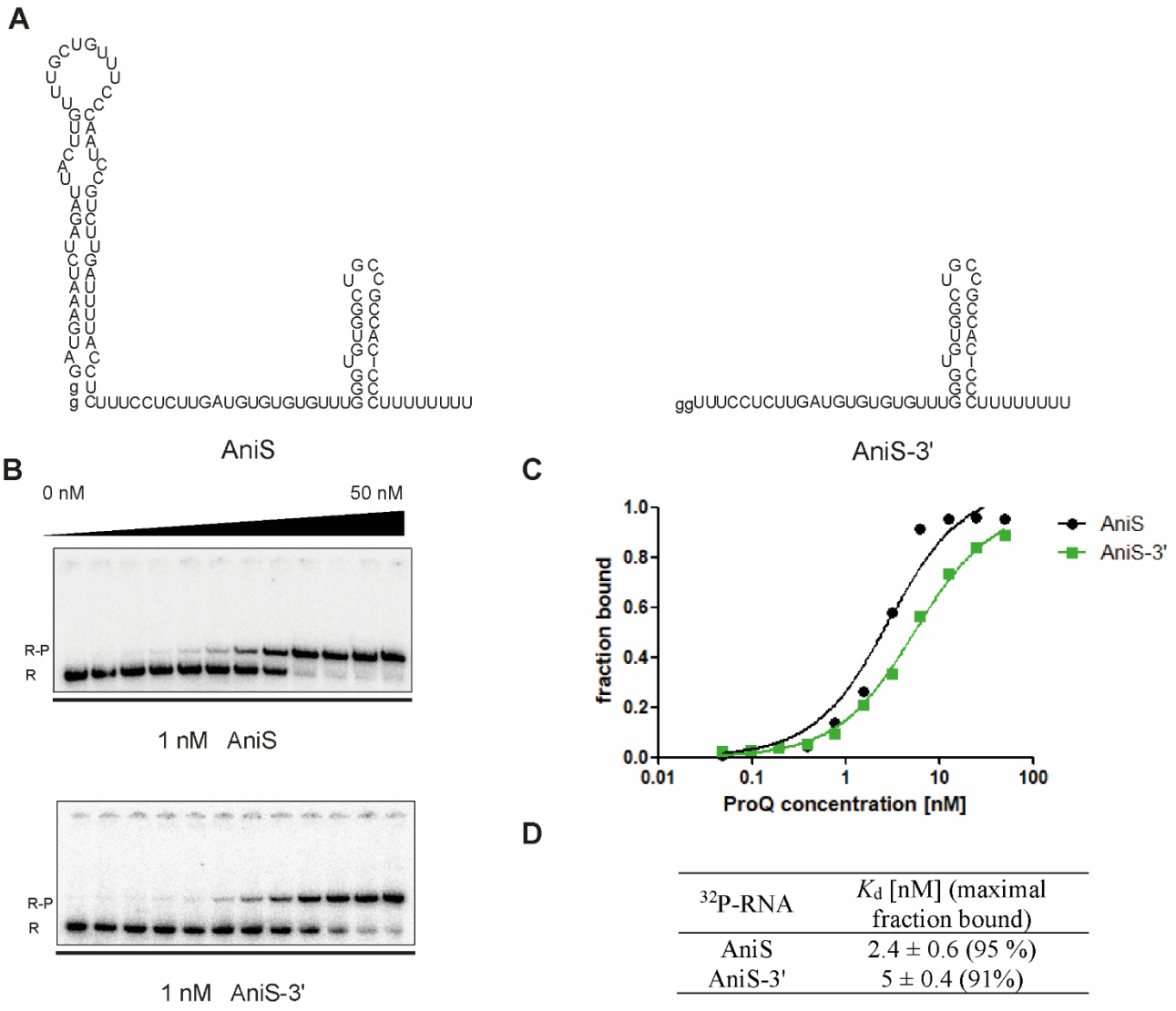

^{32}P-RNA	K_d [nM] (maximal fraction bound)
AniS	2.4 ± 0.6 (95 %)
AniS-3'	5 ± 0.4 (91%)

Supplemental Figure S2. The full-length AniS and its 3′-terminal fragment, named AniS-3′, have similar binding affinities to *N. meningitidis* ProQ. (A) Secondary structures of full-length AniS and AniS-3'. (B) The binding of ^{32}P-labeled RNAs AniS-3' and AniS was monitored using a gelshift assay. Free ^{32}P-RNA is marked as R, RNA-ProQ complexes as R-P. (C) The fitting of the ProQ binding data from B using the quadratic equation. (D) The average equilibrium dissociation constant (K_d) values and the maximum RNA fraction bound calculated from at least three independent experiments. The ProQ binding data for AniS-3′ in (C) and (D) are the same as in Figure 1 and Table 1, respectively. The RNA secondary structure predictions were performed in the *ViennaRNA* program (Lorenz et al. 2011).

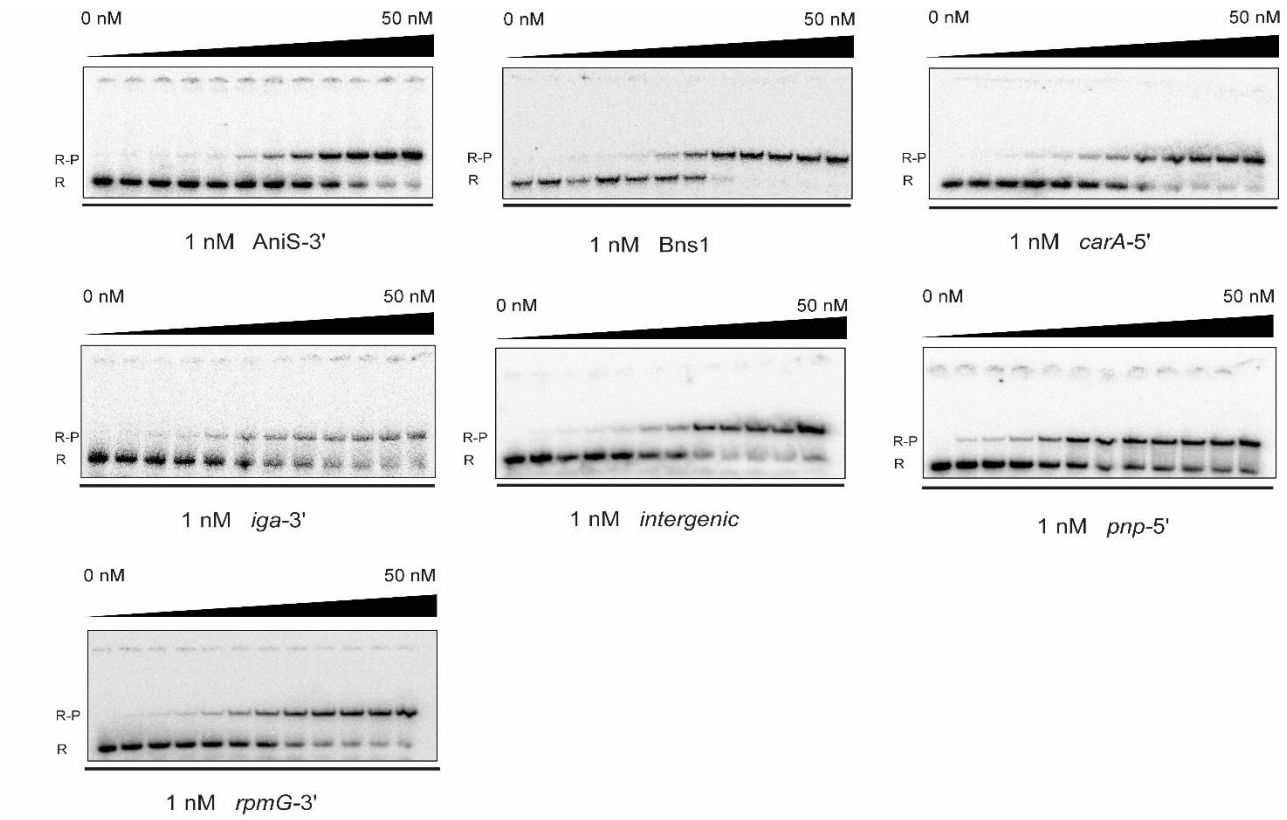

Supplemental Figure S3. Gelshift analysis of the binding of ^{32}P-labeled RNAs AniS-3', Bns1, *carA*-5', *iga*-3', *intergenic*, *pnp*-5' and *rpmG*-3' to *N. meningitidis* ProQ. The raw data in the gels correspond to the data presented in plots in Fig. 1 in the main text. The concentration series of ProQ protein was made by 2-fold sequential dilutions. The range of the ProQ concentrations is indicated above the gels. Free ^{32}P-RNA is marked as R, RNA-ProQ complex as R-P.

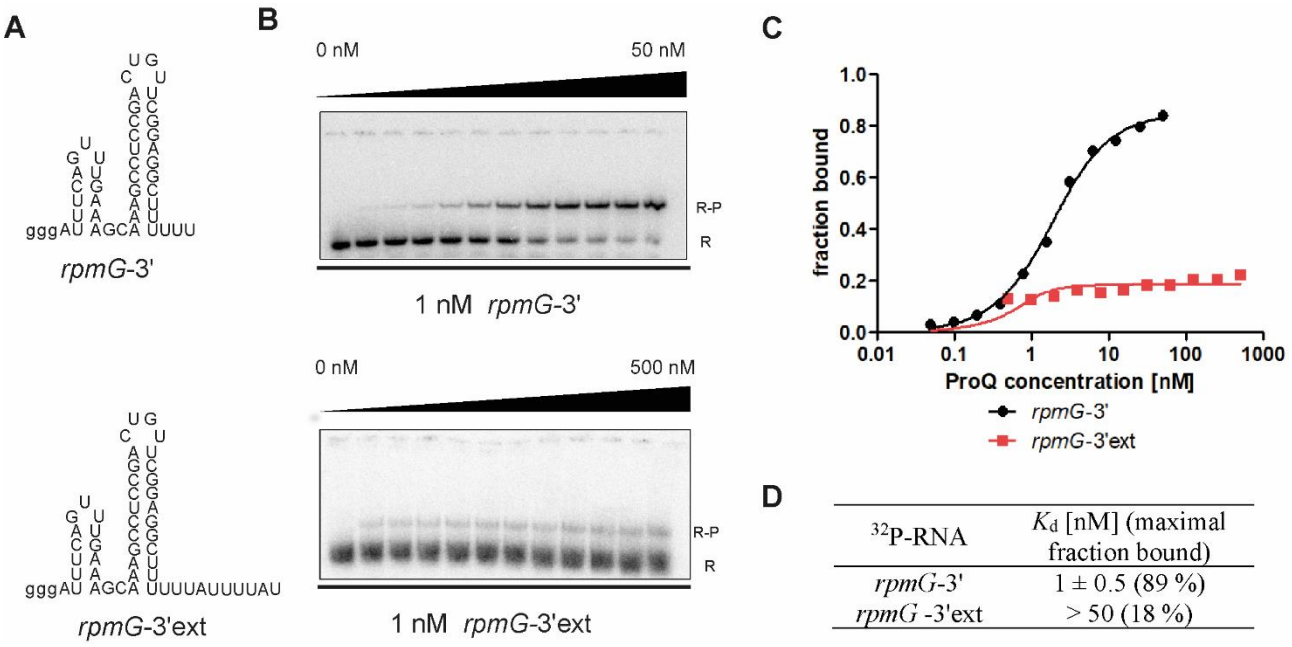

^{32}P-RNA	K_d [nM] (maximal fraction bound)
rpmG-3'	1 ± 0.5 (89 %)
rpmG -3'ext	> 50 (18 %)

Supplemental Figure S4. The 3′ extension of *rmpG*-3′ weakens its binding by *N. meningitidis* ProQ. (A) Secondary structures of *rpmG*-3' and of *rpmG*-3'ext. (B) The binding of ^{32}P-labeled RNAs *rpmG*-3' and *rpmG*-3'ext was monitored using a gelshift assay. Free ^{32}P-RNA is marked as R, RNA-ProQ complexes as R-P. (C) The fitting of the ProQ binding data from B using the quadratic equation. (D) The average equilibrium dissociation constant (K_d) values and the maximum RNA fraction bound calculated from at least three independent experiments. The ProQ binding data for *rpmG*-3′ in (C) and (D) are the same as in Figure 1 and Table 1, respectively. The RNA secondary structure predictions were performed in the *ViennaRNA* program (Lorenz et al. 2011).

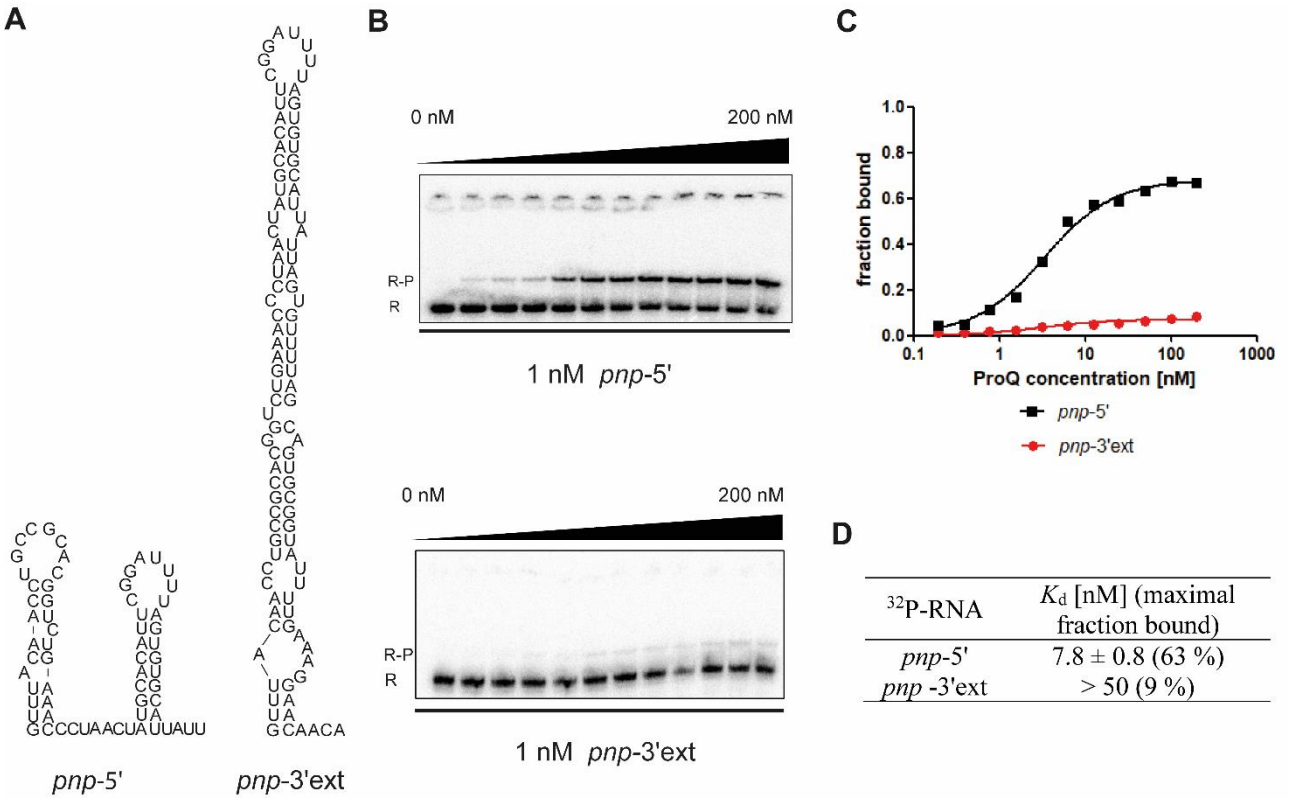

D

^{32}P-RNA	K_d [nM] (maximal fraction bound)
pnp-5'	7.8 ± 0.8 (63 %)
pnp -3'ext	> 50 (9 %)

Supplemental Figure S5. The 3′ extension of *pnp*-5' weakens its binding by *N. meningitidis* ProQ. (A) Secondary structures of *pnp*-5' and *pnp*-3'ext. (B) The binding of ^{32}P-labeled RNAs *pnp*-5' and *pnp*-3'ext was monitored using a gelshift assay. Free ^{32}P-RNA is marked as R, RNA-ProQ complexes as R-P. (C) The fitting of the ProQ binding data from B using the quadratic equation. (D) The average equilibrium dissociation constant (K_d) values and the maximum RNA fraction bound calculated from three independent experiments. The average K_d value for *pnp*-5′ is the same as in Table 1 in the main text. The RNA secondary structure predictions were performed in the *ViennaRNA* program (Lorenz et al. 2011).

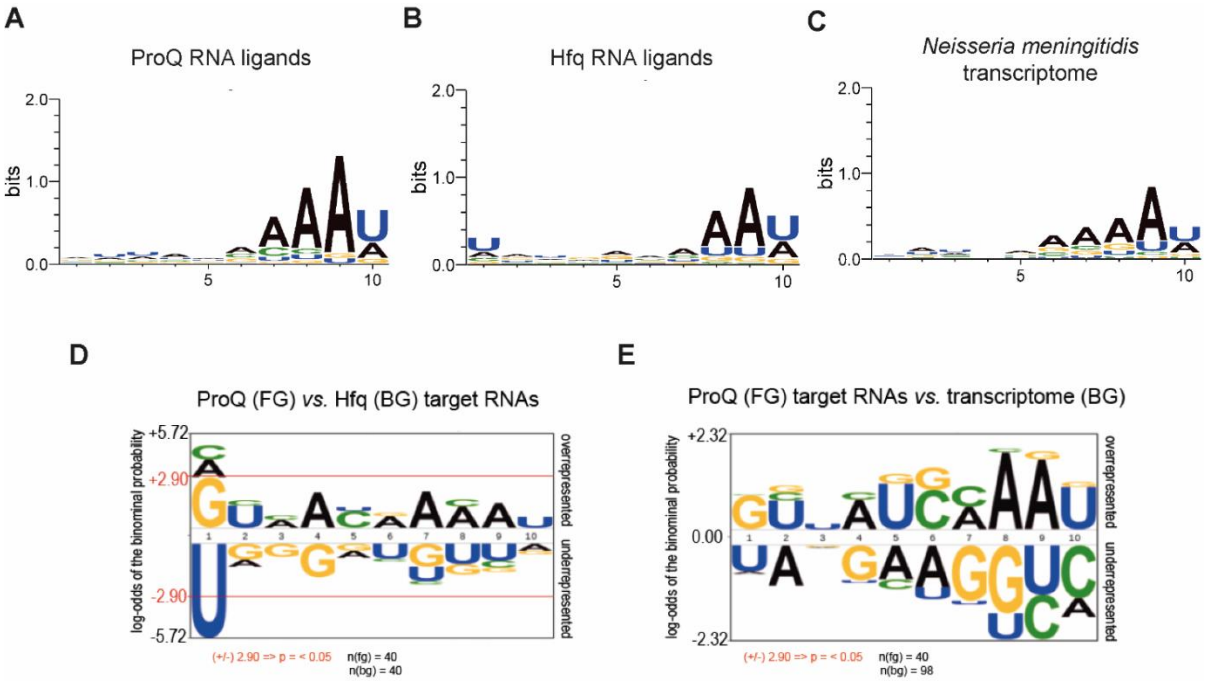

Supplemental Figure S6. The comparison of the nucleotide compositions of the 10-nt sequence on the 5' side of the closing G-C/C-G pair of the intrinsic terminator stem in RNA ligands of ProQ and Hfq, and in a random gene sample of *N. meningitidis*. Nucleotide frequencies in the 10-nt long sequence 5' adjacent to the terminator hairpin are shown for the top 40 RNA ligands of ProQ and Hfq containing Rho-independent terminators, in the data obtained previously by CLIP-seq for ProQ (Bauriedl et al. 2020) and RIP-seq for Hfq (Heidrich et al. 2017) in *N. meningitidis* (Suppl. Table S2). The last RNA ligand used for ProQ ligands logo generation (#40) corresponds to RNA positioned 74th in the CLIP-seq data set of 234 RNA ligands. The last RNA ligand used for Hfq ligands logo generation (#40) corresponds to RNA positioned 418th in the RIP-seq data set of 615 RNA ligands having logFC above 1.0. Nucleotide frequencies for *N. meningitidis* transcriptome were obtained for a random sample of 98 genes from *N. meningitidis*. (A) Nucleotide frequencies obtained by the *WebLogo* software for the top 40 *N. meningitidis* ProQ ligand RNAs containing Rho-independent terminators in CLIP-seq data. (B) Nucleotide frequencies obtained by the *WebLogo* software for the top 40 *N. meningitidis* Hfq ligand RNAs containing Rho-independent terminators in RIP-seq data. (C) Nucleotide frequencies obtained by *WebLogo* software for 98 randomly selected transcripts of *N. meningitidis*. The statistical significance of nucleotide frequencies at each nucleotide position for ProQ RNA ligands as compared to Hfq RNA ligands (D) and for ProQ RNA ligands as compared to the random sample of transcripts (E). Sequences were analysed by *pLogo* software for the top 40 *N. meningitidis* ProQ RNA ligands as the foreground, and the top 40 Hfq target RNAs or 98 gene sample from *N. meningitidis* genome as the backgrounds. Statistically significant P-value was only observed for U at position 1, P = 0.005 in ProQ ligands *vs.* Hfq ligands. The number of foreground sequences was marked on the figures as n(fg), and the number of background sequences as n(bg).

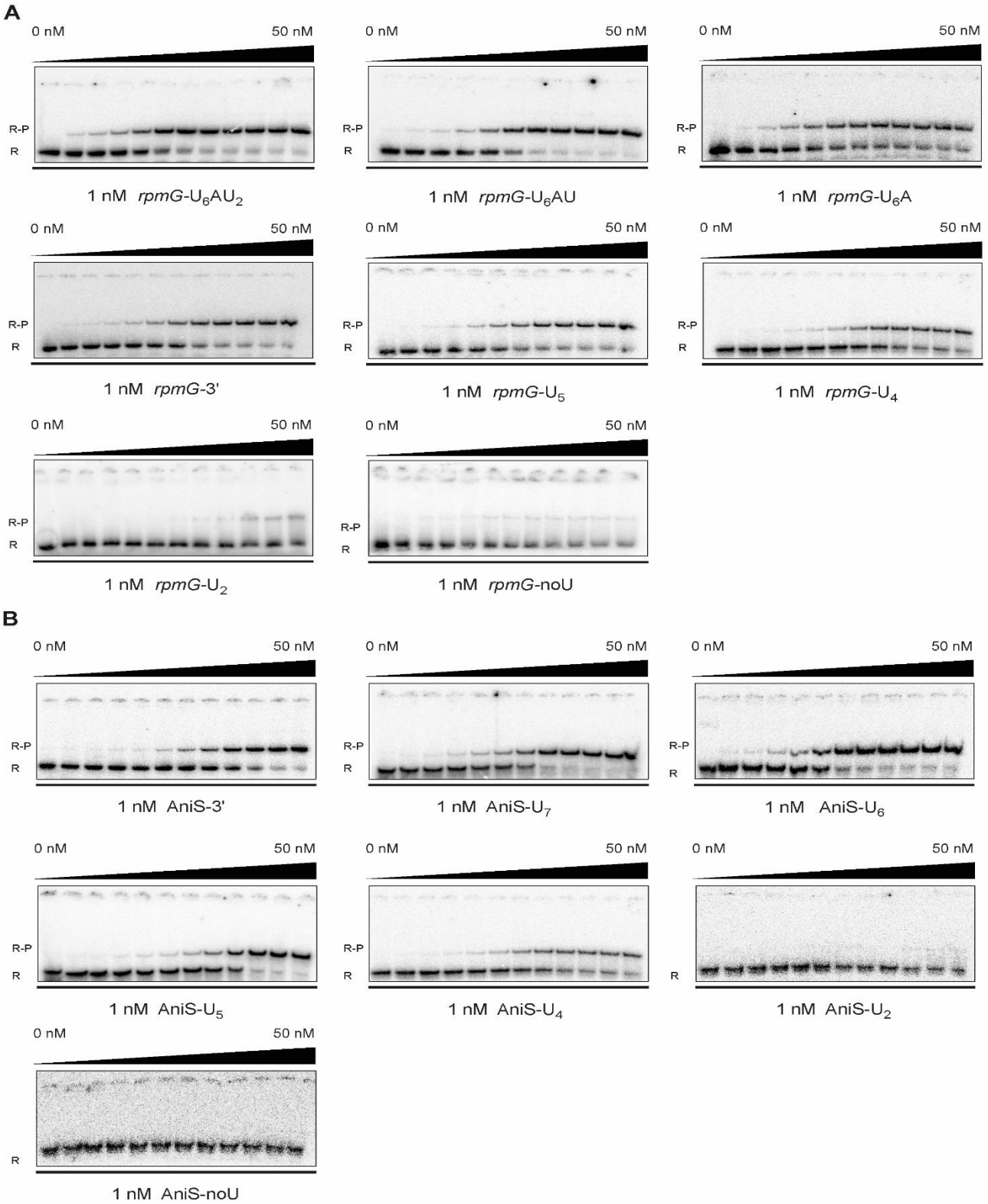

Supplemental Figure S7. Gelshift analysis of the binding of ^{32}P-labeled RNAs (A) *rpmG*-U$_6$AU$_2$, *rpmG*-U$_6$AU, *rpmG*-U$_6$A, *rpmG*-3', *rpmG*-U$_5$, *rpmG*-U$_4$, *rpmG*-U$_2$ and *rpmG*-noU, (B) AniS-3', AniS-U$_7$, AniS-U$_6$, AniS-U$_5$, AniS-U$_4$, AniS-U$_2$ and AniS-noU to *N. meningitidis* ProQ. The raw data in the gels correspond to the data presented in plots in Fig. 2 in the main text. The concentration series of ProQ protein was made by 2-fold sequential dilutions. The range of the ProQ concentrations is indicated above the gels. Free ^{32}P-RNA is marked as R, RNA-ProQ complex as R-P.

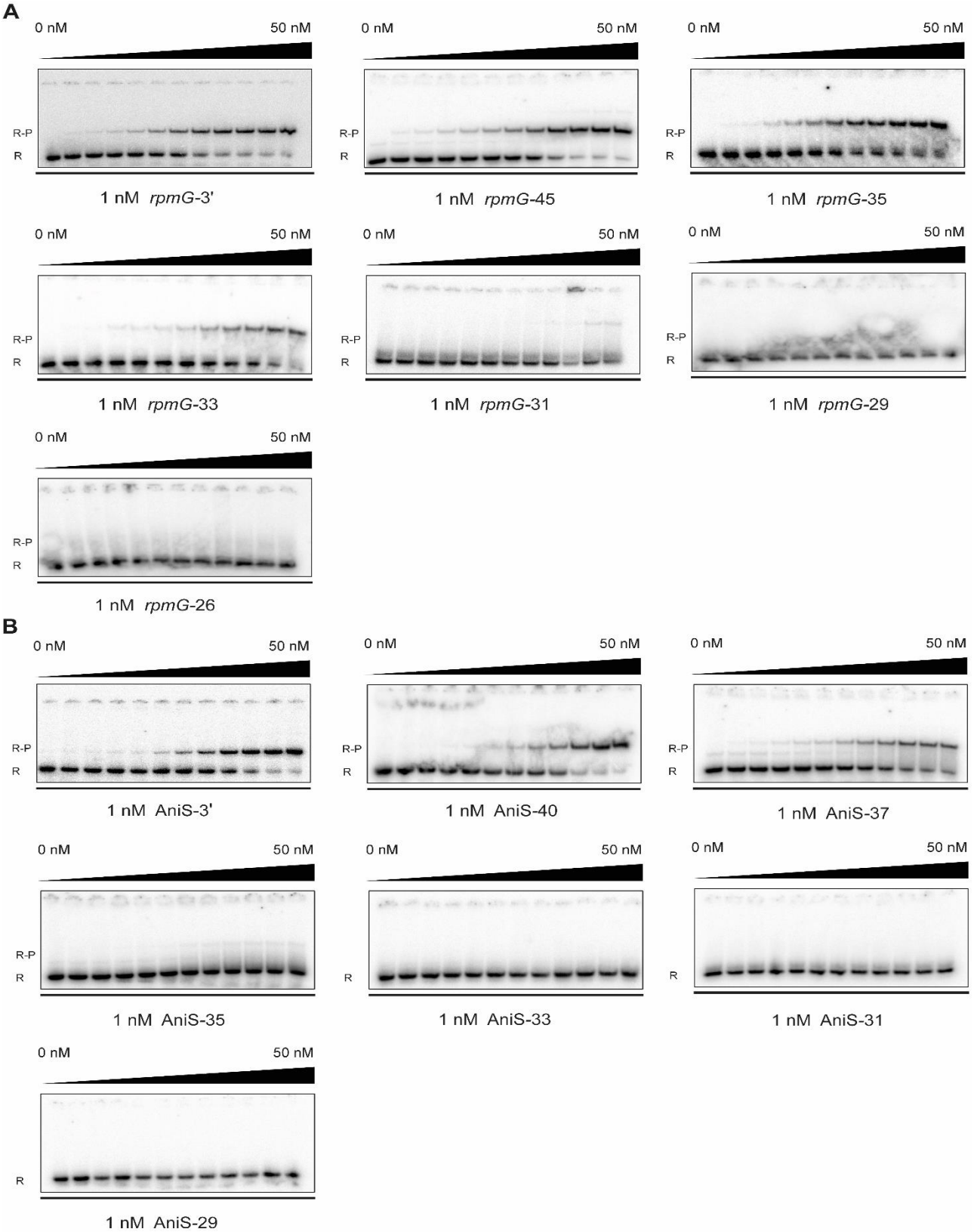

Supplemental Figure S8. Gelshift analysis of the binding of ^{32}P-labeled RNAs (A) *rpmG*-3', *rpmG*-45, *rpmG*-35, *rpmG*-33, *rpmG*-31, *rpmG*-29 and *rpmG*-26, (B) AniS-3', AniS-40, AniS-37, AniS-35, AniS-33, AniS-31 and AniS-29 to *N. meningitidis* ProQ. The raw data in the gels correspond to the data presented in plots in Fig. 3 in the main text. The concentration series of ProQ protein was made by 2-fold sequential dilutions, and its range is indicated above the gels. Free ^{32}P-RNA is marked as R, RNA-ProQ complex as R-P.

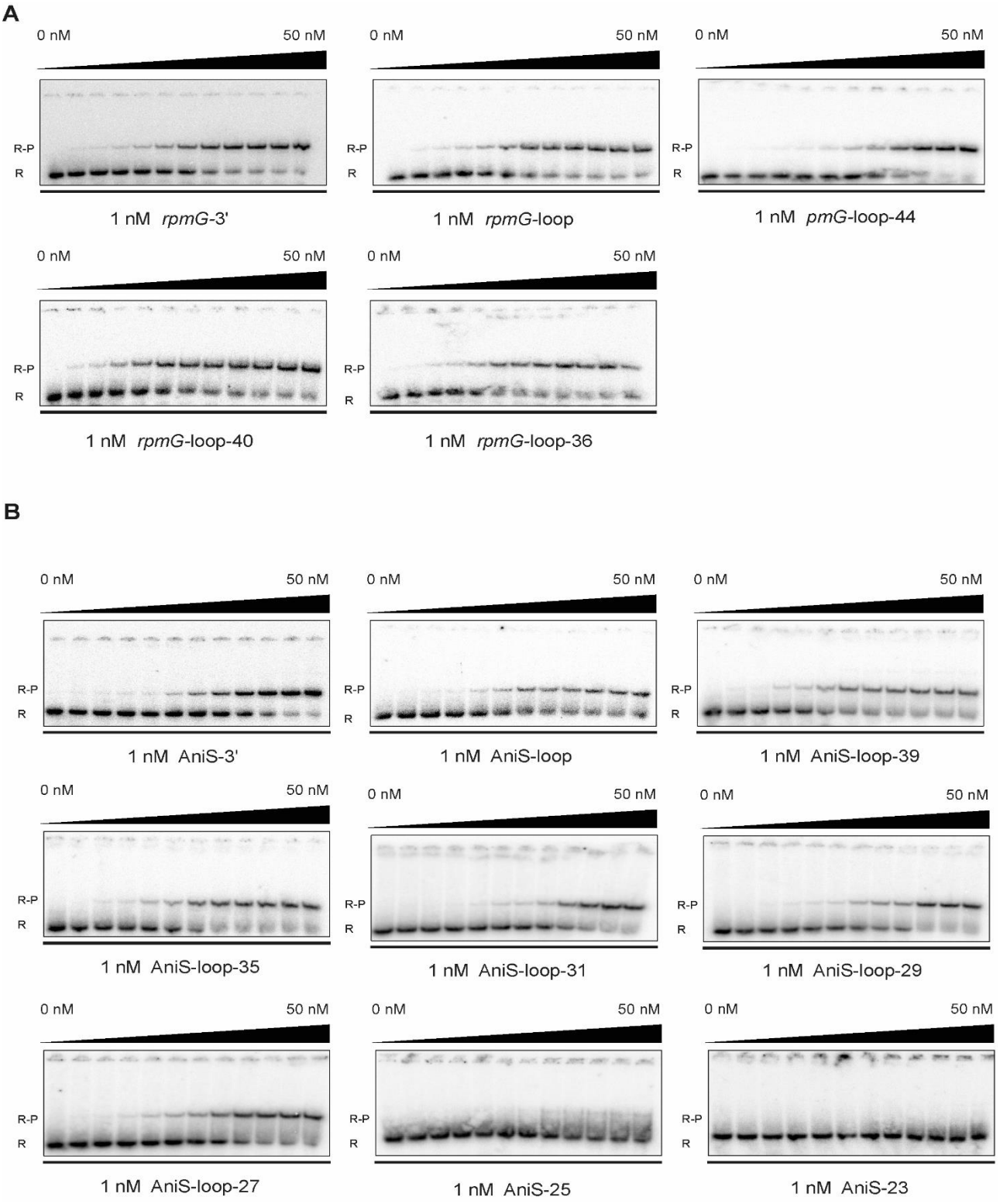

Supplemental Figure S9. Gelshift analysis of the binding of ^{32}P-labeled RNAs (A) *rpmG*-3', *rpmG*-loop, *rpmG*-loop-44, *rpmG*-loop-40 and *rpmG*-loop-36, (B) AniS-3', AniS-loop, AniS-loop-39, AniS-loop-35, AniS-loop-31, AniS-loop-29, AniS-loop-27, AniS-25 and AniS-23 to *N. meningitidis* ProQ. The raw data in the gels correspond to the data presented in plots in Fig. 4 in the main text. The concentration series of ProQ protein was made by 2-fold sequential dilutions. The range of the ProQ concentrations is indicated above the gels. Free ^{32}P-RNA is marked as R, RNA-ProQ complex as R-P.

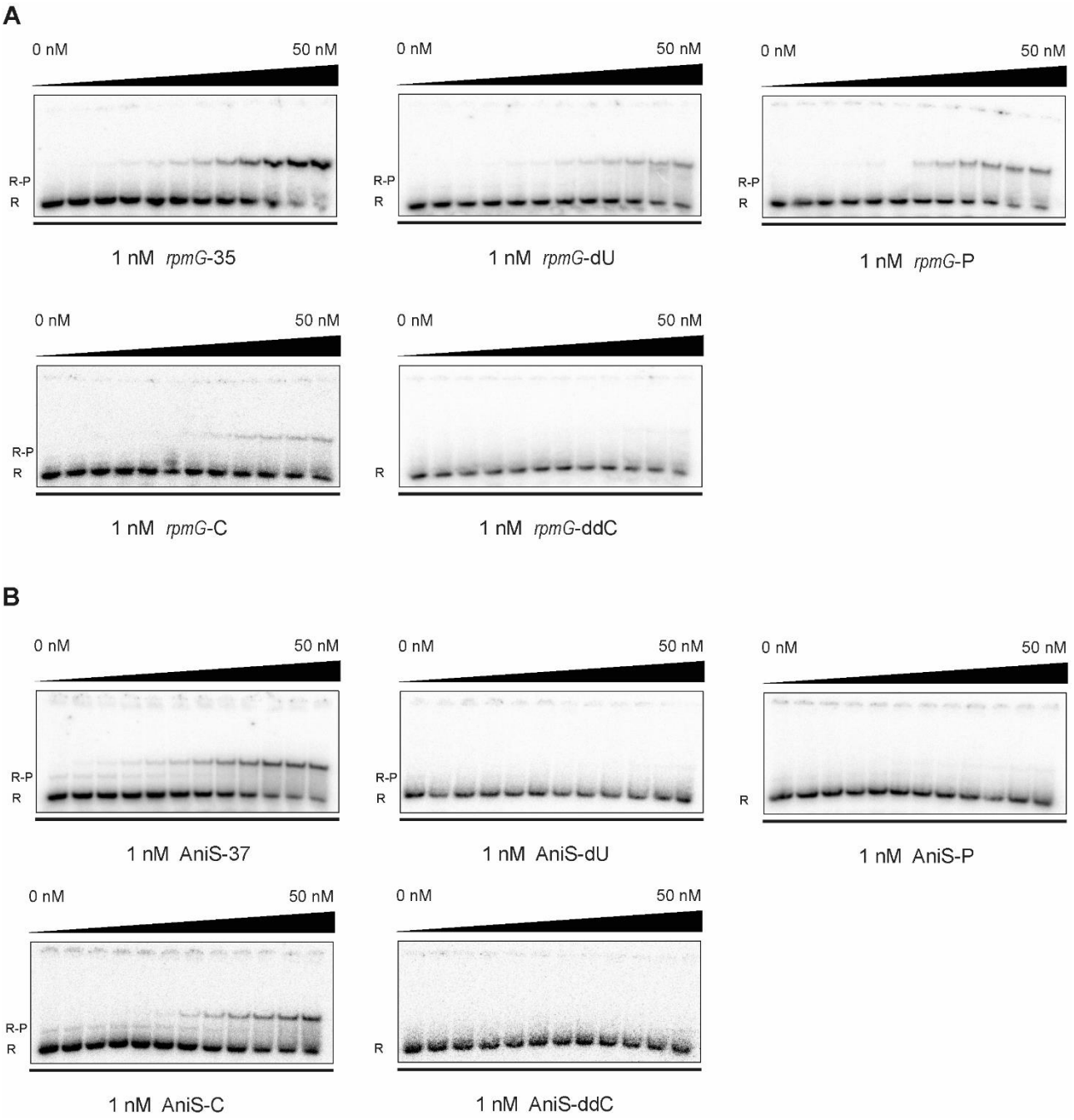

Supplemental Figure S10. Gelshift analysis of the binding of ^{32}P-labeled RNAs (A) *rpmG*-35, *rpmG*-dU, *rpmG*-P, *rpmG*-C and *rpmG*-ddC, (B) AniS-37, AniS-dU, AniS-P, AniS-C and AniS-ddC to *N. meningitidis* ProQ. The raw data in the gels correspond to the data presented in plots in Fig. 5 in the main text. The concentration series of ProQ protein was made by 2-fold sequential dilutions. The range of the ProQ concentrations is indicated above the gels. Free ^{32}P-RNA is marked as R, RNA-ProQ complex as R-P.

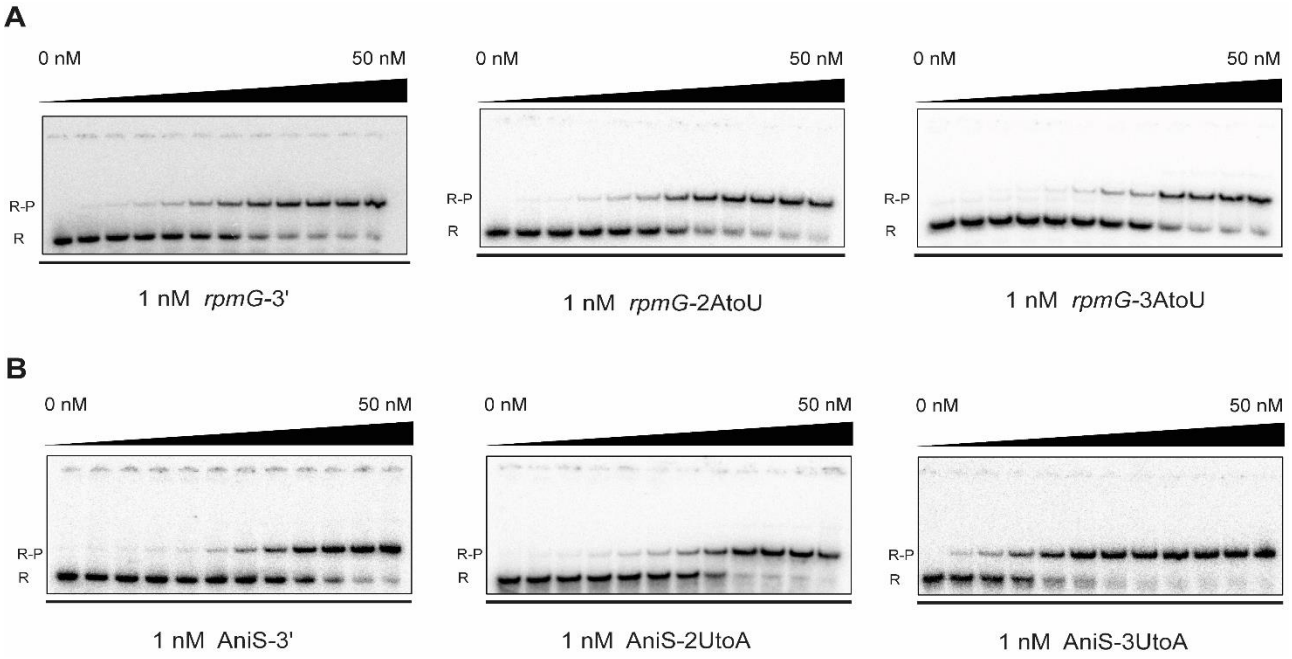

Supplemental Figure S11. Gelshift analysis of the binding of ^{32}P-labeled RNAs (A) *rpmG*-3', *rpmG*-2AtoU and *rpmG*-3AtoU, (B) AniS-3', AniS-2UtoA and AniS-3UtoA to the ProQ protein from *Neisseria meningitidis.* The raw data in the gels correspond to the data presented in plots in Fig. 6 in the main text. The concentration series of ProQ protein was made by 2-fold sequential dilutions. The range of the ProQ concentrations is indicated above the gels. Free ^{32}P-RNA is marked as R, RNA-ProQ complex as R-P.

SUPPLEMENTAL REFERENCES

Bauriedl, S., M. Gerovac, N. Heidrich, T. Bischler, L. Barquist, J. Vogel & C. Schoen (2020) The minimal meningococcal ProQ protein has an intrinsic capacity for structure-based global RNA recognition. *Nature Communications,* 11.

Crooks, G. E., G. Hon, J. M. Chandonia & S. E. Brenner (2004) WebLogo: a sequence logo generator. *Genome Res,* 14**,** 1188-90.

Heidrich, N., S. Bauriedl, L. Barquist, L. Li, C. Schoen & J. Vogel (2017) The primary transcriptome of Neisseria meningitidis and its interaction with the RNA chaperone Hfq. *Nucleic Acids Res,* 45**,** 6147-6167.

Lorenz, R., S. H. Bernhart, C. Honer Zu Siederdissen, H. Tafer, C. Flamm, P. F. Stadler & I. L. Hofacker (2011) ViennaRNA Package 2.0. *Algorithms Mol Biol,* 6**,** 26.

O'Shea, J. P., M. F. Chou, S. A. Quader, J. K. Ryan, G. M. Church & D. Schwartz (2013) pLogo: a probabilistic approach to visualizing sequence motifs. *Nat Methods,* 10**,** 1211-2.